Find the Discrepancy of the MRI Images by the Second Moment and Geometry Comparison Technique

Ching-Liang Su

Department of Industrial Engineering
Da Yeh University
112 Shan-Jeau Road, Da-Tsuen, Chang-Hua, Taiwan 51505
Tel: 886-4-852-8469 ex 2221, Fax: 886-4-852-0781
suwan@ms33.hinet.net

ABSTRACT

This research investigates the techniques using the image subtraction to find the discrepancy between the healthy and illness MRI images. The technique developed in this research moves the healthy MRI image to overlap with the illness MRI image. Then, the healthy MRI image and the illness MRI image are aligned to the same orientation. After the healthy MRI image overlapped with the illness MRI image, the illness MRI image is subtracted from the healthy MRI image. If there is discrepancy in the illness MRI image, after the image subtraction, the discrepancy will remain in the subtracted result. From beginning to end the inspection is done by the machine automatically. There is no further human effort involved. The technique developed in this research can very accurately find the discrepancy of the healthy and illness images. This paper explains the method using the second moment to find the orientations of the MRI images. By the orientations of the MRI images, the healthy MRI image and the illness MRI image can be aligned to the same orientation. The detailed process of image rotation is addressed in this paper.

Keywords: MRI image inspection, MRI image movement, image subtraction, and geometry comparison.

1. Introduction

Currently, the only efficient way to locate the MRI image discrepancy is by human beings' brains. Now, researches are trying to develop new technology to detect the discrepancy by machine. Past work in this area has used several different kinds of strategies to detect the discrepancy of the MRI image. They are - neural network [4][15], elastic frame matching [11][15], isodensity line [12], template matching [3][9][15], geometric and feature-based matching [3][10] [12], profile description [1], volumetric frequency representation [2], biometrics [6], optimal separating hyperplace [13], Gabor wavelets [14], coding representation [11], and optical network. However, some of them need a lot of computation time [9][12]; some are very sensitive to the noise [9]; some have very complicated mathematical models [12][15] and some have very complicated neural training algorithms [4][12][15]. Here, we propose a different approach, which combines several techniques, to cope with the MRI image shifting and rotating problems. Thus, after the pictures of the MRI images are taken, the algorithms developed here can automatically locate the discrepancy of the MRI images without involving further human effort. Figure 1 shows different kinds of MRI images.

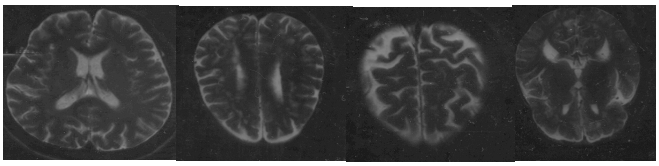

Figure 1: Different kinds of MRI images

In this research, there are two kinds of MRI images. The first kind of image is called the healthy MRI image. The second kind of image is called the illness MRI image. The healthy and illness images are shown in figure 6. The discrepancy of these two kinds of images can be detected by the technique developed in this research. Since the backgrounds are irrelevant to find the orientation and the center point of the image, the backgrounds are removed from the MRI images. The result is shown in figure 2. Major axis and centroid algorithms are used to find the orientations and the center points of these two images. Both algorithms can very precisely locate the centroids and orientations of these MRI images. This research only processes the two

dimensional images. The three dimensional images are not investigated in this research. This research first shifts the healthy MRI image to make the centroid of the healthy MRI image to overlap with the centroid of the illness MRI image. Then, the healthy MRI image is rotated. Thus, the healthy MRI image can be aligned to the same orientation as the illness MRI image. After this, image subtraction can be applied to these two MRI images. The subtracted result can very precisely show the discrepancy of these two MRI images. Under normal circumstance, when the MRI images are taken, even though the MRI image are a little shifted or a little rotated, the algorithms developed in this research will still correctly find the discrepancy of the healthy and illness MRI images.

This paper consists of five sections. Section 2 discusses how to extract the important feature of the MRI images. Section 3 explains how to find the centroids and orientations of the MRI image. Section 4 performs the image subtraction. Section 5 concludes this paper.

2. MRI Image extraction

In order to find the locations and orientations of the MRI images, the important feature of MRI images must be extracted. In previous investment, a lot of work about the object enhancement and object extraction research is developed. In many cases, the image extracting technique can work well to extract the feature of the object. In this research, we do not deal with the object extraction process. Instead, the technique, which provided by the other researcher, is used to extract the object. The extracted images are shown in the following graph.

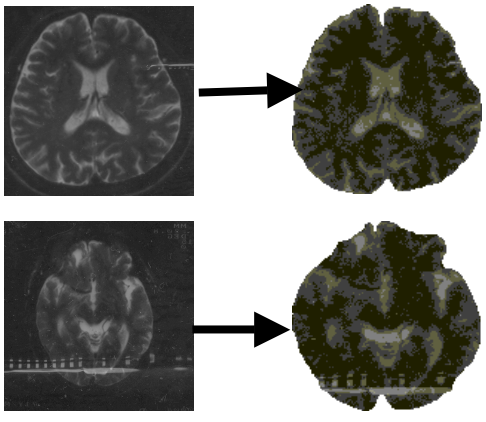

Figure 2: The extracted image

3. Finding the centroid and orientation of an extracted MRI object

3.1. Finding the centroid

The size of the image used in this research is 128*128 image array. The centroid (x_c, y_c) of an image can be found by the following equations:

$$m_{pq} = \int\int x^p y^q b(x,y)dxdy$$

$$u_{pq} = \int\int (x-x_c)^p (y-y_c)^q b(x,y)dxdy$$

$$x_c = \frac{m_{10}}{m_{00}} = \frac{\int\int xb(x,y)dxdy}{\int\int b(x,y)dxdy} \quad (1)$$

$$x_c \int\int b(x,y)dxdy = \int\int xb(x,y)dxdy$$

$$y_c = \frac{m_{10}}{m_{00}} = \frac{\int\int yb(x,y)dxdy}{\int\int b(x,y)dxdy} \quad (2)$$

$$y_c \int\int b(x,y)dxdy = \int\int yb(x,y)dxdy$$

In the above equations, *b(x, y)* represents the gray level on location *(x, y)*; (x_c, y_c) represents the centroid of the MRI image.

3.2. Using the second moment to find the orientation of the MRI image[7]

The major axis is the axis around which the object will have the minimum moment of inertia. This is useful in determining the object's orientation. The following graph shows the object major axes:

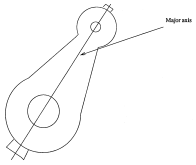

Figure 3: Construction for showing the object major axis.

Figure 4 shows the relative position of the major axis. The major axis and X-axis generate an angle θ. The shortest distance from the origin to the major axis is t. The major axis and X-axis intersect at the point (-t/sin θ, 0). The major axis and Y axis intersect at the point (0 , t/cos θ). The point inside the major axis which has the minimum distance to the origin is (-t*sin θ, t*cos θ).

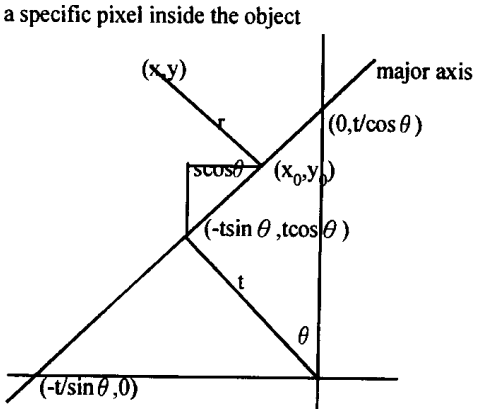

Figure 4: The relative position of the major axis.

By analyzing figure 4, the equation for the major axis can be expressed as:

$$x(\sin\theta)-y(\cos\theta)+t=0 \quad (3)$$

In figure 4, suppose one specific point (x_0,y_0) is located inside the major axis. From point (x_0,y_0) to point $(-t*\sin\theta, t*\cos\theta)$, the distance is s. From figure 4, one can find:

$$x_0=-t(\sin\theta)+s(\cos\theta) \quad (4)$$

$$y_0=+t(\cos\theta)+s(\sin\theta) \quad (5)$$

Given a point (x,y) on the object, r is the shortest distance between (x,y) and (x_0,y_0). Clearly,

$$r^2=(x-x_0)^2+(y-y_0)^2 \quad (6)$$

Equation (4) and (5) are substituted into equation (6). The obtained result is differentiated with respect to s. Setting the result equal to zero, the following equation can be obtained.

$$s=x(\cos\theta)+y(\sin\theta) \quad (7)$$

$$r=(x(\sin\theta)-y(\cos\theta)+t) \quad (8)$$

The second moment, which describes the object, is:

$$E=\iint r^2 b(x,y)\,dx\,dy \quad (9)$$

r is the distance of one specific pixel inside the object to the major axis. However, the distance is the minimum. b(x,y) is the gray level of pixel at location (x,y).

By analyzing equation (1), (2), and (9), the following equations can be derived:

$$E=(1/2)(a+c)-(1/2)(a-c)(\cos2\theta)-(1/2)(b)(\sin2\theta) \quad (10)$$

Differentiate with respect to θ and set the differentiating result to 0, the following equation can be obtained:

$$\tan2\theta=b/(a-c) \quad (11)$$

The values of a, b, c, and θ can be found for any images. The θ will represent the angle of the major axis with respect to the x axis. Based on θ, the algorithm can find the orientation of the object. The above second moment equation which to find the object orientation can be summarized as the following equation:

$$a=\int\int (x')^2 b(x,y)\,dx\,dy$$

$$b=2\int\int (x'y')b(x,y)\,dx\,dy$$

$$c=\int\int (y')^2 b(x,y)\,dx\,dy$$

$$tan2\theta=\frac{b}{a-c}$$

$$sin2\theta=\frac{+}{-}\frac{b}{(b^2+(a-c)^2)^{\frac{1}{2}}}$$

$$cos2\theta=\frac{+}{-}\frac{a-c}{(b^2+(a-c)^2)^{\frac{1}{2}}}$$

4. Geometry comparison of the MRI image

4.1. MRI image shifting and rotating

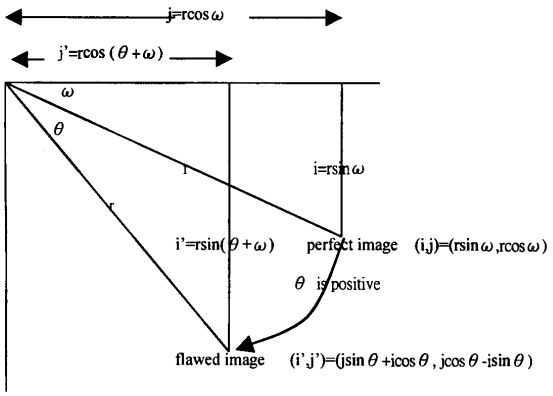

Figure 5: Show the corresponding position after the perfect (healthy) image is rotated θ degrees toward the flawed (illness) image.

Using the method described in the previous section, the orientation of each extracted MRI image can be found. In this research, there are two kinds of images: the perfect (healthy) image and the flawed (illness) image. The healthy and illness images are shown in the following graphs:

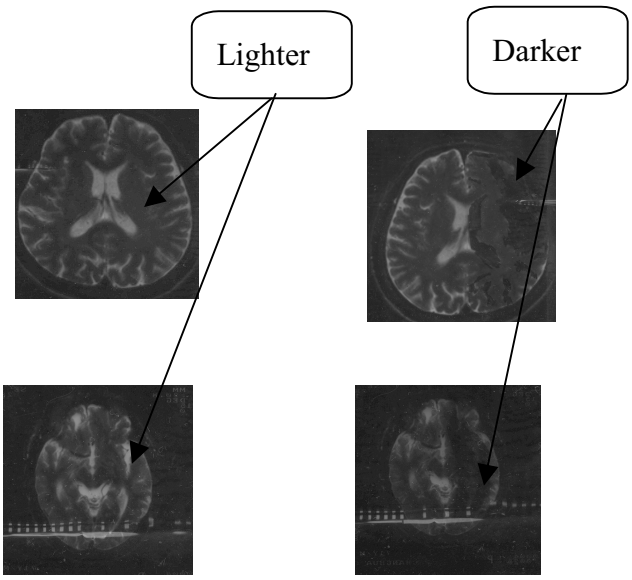

Figure 6: Show the healthy MRI image and the illness MRI image

The MRI images in (b) and (d) in the right parts are darker than the right part images, which (a) and (c) have.

As mentioned before, in order to overlap the healthy image with the illness image, the healthy image needs to be shifted and rotated. In this section, the image shifting and image rotation is addressed.

$i'=j\sin\theta+i\cos\theta$, and
$j'=j\cos\theta-i\sin\theta$
can be obtained. If the rotated direction is clockwise, then θ is positive; otherwise, θ is negative.

By analyzing figure 5, equation (12) can be obtained. This means that the healthy image is translated so that the centroid is moved to the origin of the coordinate. Next the picture is rotated so that the healthy image is at the same orientation as the illness image. Finally the picture is translated so that the healthy image centroid and illness image centroid are overlapping each other. The equation, which carries out these operations, is shown in equation (13). Equation (13) will combine both the image rotation and image translation in one step. By using equation (13), the algorithm can rotate and transfer the healthy image point (i,j) to its proper position (i_f,j_f). (i_f,j_f) represents the position in the illness image which corresponds to the position (i,j) in the healthy image.

4.2. Interpolating the non-integer point

In this research, there are two kinds of image movement: image translation and image rotation. Simply shifting the pixels inside the healthy image so that the centroid of the healthy image is overlapping the origin of the coordinate does image translation. After performing image translation, the location of pixels in the healthy image may have non-integer values.

$$\begin{bmatrix} i_f \\ j_f \\ 1 \end{bmatrix} = \left(\begin{bmatrix} 1 & 0 & knowni \\ 0 & 1 & knowij \\ 0 & 0 & 1 \end{bmatrix} * \left(\begin{bmatrix} \cos\theta & \sin\theta & 0 \\ -\sin\theta & \cos\theta & 0 \\ 1 & 0 & 1 \end{bmatrix} * \left(\begin{bmatrix} 1 & 0 & -testi \\ 0 & 1 & -testj \\ 0 & 0 & 1 \end{bmatrix} * \begin{bmatrix} i \\ j \\ 1 \end{bmatrix} \right) \right) \right) \qquad (12)$$

$$\begin{bmatrix} i_f \\ j_f \\ 1 \end{bmatrix} = \begin{bmatrix} (i-testi)\cos\theta + (j-testj)\sin\theta + knowni \\ -(i-testi)\sin\theta + (j-testj)\cos\theta + knownj \\ 1 \end{bmatrix} \qquad (13)$$

Figure 5 shows the corresponding position after the healthy image is rotated θ degrees toward the illness image. (i, j) is the location of one specific pixel which is located inside the healthy image. The point (i,j), after being rotated θ degrees, will move the position to (i',j'). Clearly, from figure 5, one can find $i=r\sin\omega$, $j=r\cos\omega$, $i'=r\sin(\theta+\omega)$, and $j'=r\cos(\theta+\omega)$. Since
$\sin(\theta+\omega)=\sin\theta\cos\omega+\cos\theta\sin\omega$, and
$\cos(\theta+\omega)=\cos\theta\cos\omega-\sin\theta\sin\omega$, the equations

After performing image rotation, the new position of a pixel might not be represented by integers, either. The relative position of the sub-pixel *(i,j)* is shown in the following graph:

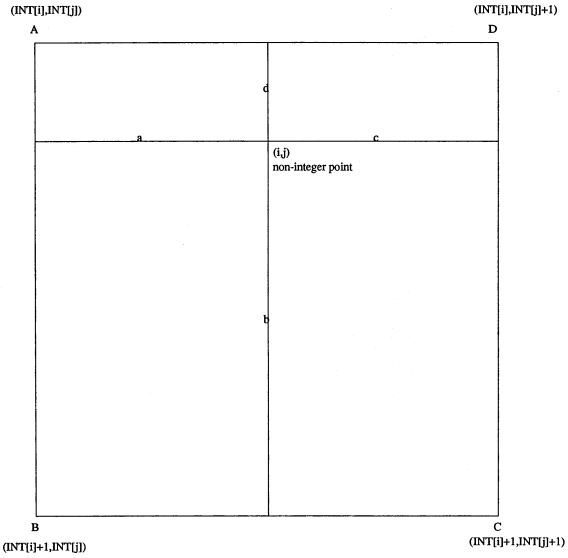

Figure 7: Show the relative position of the sub-pixel (i,j)

To directly compare pixels from the healthy image to pixels from the illness image, it is necessary to find values for pixels in the healthy image at the same points (integer values) as those in the illness image. The non-integer coordinate positions, which are obtained from the calculation of the mathematical function 13, have different distances to their four neighboring integer pixels. The gray level of these non-integer points need to be interpolated from their four neighboring integer pixels in order to obtain their proper gray level values.

4.3. Geometry comparison

After the image interpolation, the illness and healthy images lie in the integer points. Both images have the same orientation. The centroids of both images are overlapped. Image subtraction can now be applied to both images.

5. Results and conclusions

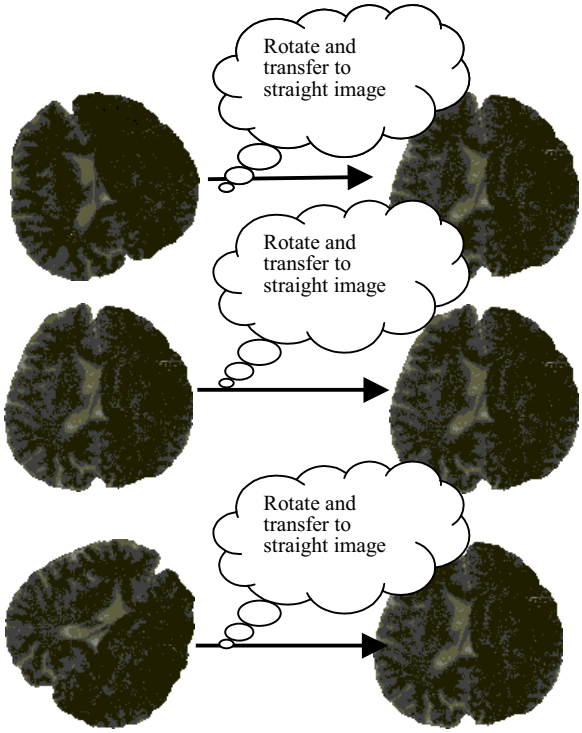

Figure 8: The illness MRI images are rotated and transferred. The illness MRI images is moved to the same orientation and centroid, which the healthy MRI image has

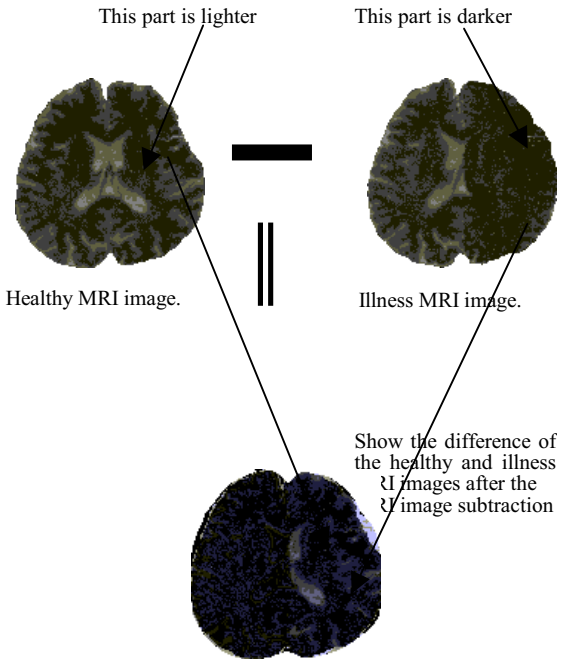

Figure 9: The healthy and illness images are overlapped and subtracted.

Since one can find the centroid and orientation of the MRI image, by using the previous mentioned rotating, transferring, and interpolating technique, the illness MRI image can be aligned to the same orientation as the healthy image. The rotated and shifted images are shown in figure 8.

After the transferring, the image subtraction is performed to both images. The subtracted image is show in figure 9. In this case, since the illness image in the right-hand side is darker than the corresponding right-hand side portion of the healthy MRI image, after the subtraction, the subtracted result in figure 9 is not totally blacks. As we can see, in the final result of figure 9, the right-hand side portion of this subtracted image has the light spots in there. These light spots show the discrepancy of the healthy and illness MRI images.

By this result, one can find that the technique developed in this research can work well to find the discrepancy between the healthy and illness MRI images.

References

[1] T. Aibara, k. Ohue, and Y. Oshita, "Human Face Profile Recognition by a P-Fourier Descriptor", Optical Eng., Vol.32, No. 4, April 1993, pp 861-863.

[2] J. BenArie and D. Nandy, "A Volumetric/Iconic Frequency Domain Representation for Objects with Application for Pose Invariant Face Recognition", IEEE Trans. on Patt. Anal. and Machine Intell., Vol. 20, No. 5, May 1998, pp 449-457.

[3] R. Brunelli and T. Poggio, "Face Recognition: Features versus Templates", IEEE Trans. on Patt. Anal. and Machine Intell., Vol. 15, No. 10, Oct. 1993, pp 1042-1052.

[4] Minoru Fukumi, Sigeru Omatu, Fumiaki Takeda, and Toshihisa Kosaka, "Rotation-Invariant Neural Pattern Recognition System with Application to Coin Recognition", IEEE Transactions on Neural Networks, Vol.3, No.2, March 1992, pp272-279

[5] R. Gonzalez and P. Wintz, "Digital Image Processing", Addison-Wesley Publishing Company, Mass., 1977.

[6] L. Hong and A. Jain, "Integrating Faces and Fingerprints for Personal Identification", IEEE Trans. on Patt. Anal. and Machine Intell., Vol. 20, No. 12, Dec. 1998, pp 1295-1307.

[7] B. K. P. Horn, "Robot Vision", McGraw-Hill Book Co., New York, pp. 49-53, 1986.

[8] M. Kamel, H. Shen, A. Wang, and R. Campeanu, "System for Recognition of Human Faces", IBM System J., Vol.32, No. 2, 1993, pp 307-320.

[9] S. Karbacher, "Associative Object Recognition by Hierachic Template Matching", Optical Eng., Vol. 29, No. 12, Dec. 1990, pp 1449-1457.

[10] K. Lam and H. Yan, "An Analytic–to-Holistic Approach for Face Recognition Based on a Single Frontal View", IEEE Trans. on Patt. Anal. and Machine Intell., Vol. 20, No. 7, July 1998, pp 673-686.

[11] A. Lanitis, C. Taylor, and T. Cootes, "Automatic Interpretation and Coding of Face Image Using Flexible Models", IEEE Trans. on Patt. Anal. and Machine Intell., Vol. 19, No. 7, July 1997, pp 743-756.

[12] O. Nakamura, S. Mathur, and T. Minami, "Identification of Human Faces Based on Isodensity Maps", Patt. Recog., Vol. 24, No. 3, 1991, pp 263-272.

[13] M. Pontil and A. Verri, "Support Vector Machines for 3D Object Recognition", IEEE Trans. on Patt. Anal. And Machine Intell., Vol. 20, No. 6, June 1998, pp 637-646.

[14] L. Wiskott, J. Fellous, NorberKr, and C. Malsburg, "Face Recognition by Elastic Bunch Graph Matching", IEEE Trans. on Patt. Anal. and Machine Intell., Vol. 19, No. 7, July 1997, pp 775-779.

[15] A. Yuille, P. Hallinan, and D. Cohen, "Feature Extraction from Faces Using Deformable Templates", Int. J. of Comput. Vision, 8:2, 1992, pp 99-111.